Available online at www.sciencedirect.com
SCIENCE DIRECT®

Polymer 45 (2004) 1617–1626

polymer

www.elsevier.com/locate/polymer

Solid polymer electrolytes VIII: effect of $LiClO_4$-doped level on the microstructure and ionic conductivity of a chemical-covalently polyether-siloxane hybrid electrolyte

Wuu-Jyh Liang, Ping-Lin Kuo*

Department of Chemical Engineering, National Cheng Kung University, Tainan 70101, Taiwan, ROC

Received 23 May 2003; received in revised form 14 October 2003; accepted 15 December 2003

Abstract

A new hybrid polymer electrolyte system based on chemical-covalently polyether and siloxane phases is designed and prepared in the presence of lithium perchlorate ($LiClO_4$) which acted as both ionic source and the epoxide ring-opening catalyst. The effect of salt-doped level on the microstructure and ionic conductivity of these composite electrolytes were investigated by means of Fourier transform infra-red spectroscopy, differential scanning calorimetry (DSC), thermogravimetric analysis, a.c. impedance and multinuclear solid-state nuclear magnetic resonance measurements. DSC results indicate that the formation of transient cross-links between Li^+ ions and the ether oxygens on complexation with $LiClO_4$ results in an increase in polyether segment T_g. However, the polyether segment T_g decreases at the highest salt concentration (5.0 mmol $LiClO_4$/g PEGDE), ascribing to the plasticizing effect. The behavior of ion transport is coupled with the segmental motions of polymer chains and also correlated with the interactions between ions and polymer host.

Keywords: Hybrid electrolyte; Microstructure; Ionic conductivity

1. Introduction

Solid polymer composite electrolytes have attracted widespread interest in recent years due to their potential industrial applications, namely, in solid-state rechargeable batteries, fuel cells, sensors, electrochromic display devices, and super capacitors [1–3]. The family of poly(ethylene oxide) (PEO) polymers has been extensively studied because of its solvation power and complexing ability to alkali metal ion. While PEO chains act as solid solvents for many lithium salts, the limited conductivity at room temperature, low processability, and poor mechanical properties limit their practical uses [4]. It is well established [5–7] that ion conduction takes place predominantly in the amorphous region, and that high segmental mobility of the polymers corresponding to low glass transition temperature (T_g) ensures high mobility of the dissociated ions. The increasing volume fraction of the amorphous domains and the decreasing T_g appear to be the main path toward obtaining better ionic conductivity.

Recently, considerable advance has been gained by designing new polymer electrolytes based on organic–inorganic hybrids or nanocomposite systems [8–10], among which silica-based materials hold a prominent place. A variety of organic–inorganic hybrids presenting covalent bonds or only weak physical bonds (hydrogen bonding or van der Waals bonds) between the inorganic (siloxane) and organic (polymer) phases have been proposed [11–15]. These solid electrolytes are now widely known as ormolytes (an abbreviation of *or*ganically *mo*dified electro*lytes*) and their properties strongly depend on the connectivity of the inorganic–organic phases and the mobility of both structural network and active species [16–20].

In an effort to design a new class of organic–inorganic hybrid electrolyte consisting of completely amorphous phase and possessing excellent mechanical property, in this study, the polyether-siloxane-$LiClO_4$ hybrids with covalent bonds between the organic polymer chains and the siloxane phase are prepared using lithium perchlorate ($LiClO_4$) as oxirane ring-opening catalyst. These hybrid

---

* Corresponding author. Tel.: +886-6-275-7575; fax: +886-6-276-2331. *E-mail address:* plkuo@mail.ncku.edu.tw (P.L. Kuo).

0032-3861/$ - see front matter © 2003 Elsevier Ltd. All rights reserved.
doi:10.1016/j.polymer.2003.12.057

electrolytes are based on blending poly(ethylene glycol) diglycidyl ether (PEGDE) with 3-glycidoxypropyltrimethoxysilane (GPTMS) and $LiClO_4$, in which $LiClO_4$ also acts as ionic source. Multinuclear solid-state nuclear magnetic resonance (NMR) spectroscopy is used to provide information about the microscopic structure and molecular behavior; complex impedance measurement is used to describe the ionic conductivity properties; differential scanning calorimetry (DSC) further evidences for phase transitions in these composite polymer electrolytes; thermogravimetric analysis (TGA) characterizes the thermal stability. These results are correlated and found that the $LiClO_4$-doped level significantly affects the microscopic structure, molecular behavior and ion conduction of the resulted hybrid materials.

2. Experimental

2.1. Materials

Poly(ethylene glycol) diglycidyl ether (PEGDE, EEW = 290 g/equiv., Kyoeisha Chemical Co., Ltd) was dehydrated at 80 °C under vacuum for 72 h prior to use. Lithium perchlorate ($LiClO_4$, Aldrich) was dried at 120 °C under vacuum for 72 h. 3-Glycidoxypropyltrimethoxysilane(GPTMS, Dow Corning Corporation), tin-catalyst (M and T Fastcat 4200 catalyst) and acetone (Alps) were used as received.

2.2. Sample preparation

PEGDE and GPTMS were mixed with a desired weight ratio in acetone at room temperature, and then tin-catalyst (0.1 wt% based on the weight of GPTMS) as well as the desired amounts of lithium perchlorate was added. After vigorous stirring, the mixture was then cast onto aluminum plate, and followed by slowly removing the solvent at room temperature, cured at 100 °C for 24 h and 150 °C for 2 h to form an inter-crosslinked hybrid material. The thickness of these specimens was controlled to be in the range of 150–200 μm. The hybrid materials were dried under vacuum at 80 °C for 72 h until no weight loss observed, and then stored in an argon-filled glove box (Vacuum Atmosphere, USA) for cell assembly. The concentration of $LiClO_4$ in the organic–inorganic hybrid networks was represented by the amount of $LiClO_4$ (in mmole) per gram of PEGDE or the molar ratio of ether oxygen to $LiClO_4$ ($[O]/[Li^+]$) (see Table 1).

2.3. Characterizations

Fourier transform infra-red (FT-IR) spectra were measured by using a Nicolet 550 system with a wavenumber resolution of 2 cm^{-1}, and a minimum of 64 scans was signal-averaged at room temperature under dry nitrogen atmosphere. Each sample was prepared by mixing with potassium bromide (KBr) pellet, and films were vacuum-dried at 80 °C for several days to remove the absorbed water in the sample.

Table 1
DSC results for PEGDE-GPTMS-$LiClO_4$ with various addition of salt

mmol $LiClO_4$/g PEGDE	O/Li^+	T_{g1} (°C)	ΔT_{g1} (°C)	T_{g2} (°C)	T_{mc} (°C)[a]
0.1	200	−31.8	13.8		111.1
1.0	20	−31.0	10.4	43.2	125.1
2.0	10	−24.8	11.6	42.7	144.1
3.0	7	−20.7	12.8	45.8	147.5
5.0	4	−34.5	14.1	54.3	148.6

[a] T_{mc} : The melting point of crystalline PEG-$LiClO_4$ complex phase.

TGA analysis were carried out using a thermogravimetric analyzer (Perkin–Elmer TGA 7) over a temperature range of 100–800 °C at a heating rate of 20 °C/min under nitrogen atmosphere.

DSC data were recorded between −150 and +200 °C using a DuPont TA2010 differential scanning calorimeter with a low-temperature measuring head and a liquid nitrogen-cooled heating element. Samples in aluminum pans were stabilized by slow cooling to −150 °C and then heated at 10 °C/min to +200 °C. The glass transition zone was determined as the temperature range between two intersection points of the base lines with the extrapolated sloping portion of the thermogram, which resulted from a heat capacity change. Glass transition temperatures (T_g) were reported as the midpoint of the transition process. All the thermograms were baseline corrected and calibrated against indium metal. An empty aluminum pan was used as a reference.

High-resolution solid-state NMR experiments were carried out on a Bruker AVANCE 400 spectrometer, equipped with a 7 mm double-resonance probe. The Larmor frequencies for ^1H, ^7Li, and ^{13}C nuclei are, respectively, 400.17, 155.45, and 100.58 MHz. Magic angle spinning (MAS) of the samples in the range of 3–5 kHz was employed for obtaining NMR spectra. The Hartmann–Hahn condition for $^1H \rightarrow {}^{13}C$ cross-polarization (CP) experiments was determined using admantane, and proton decoupling was applied during acquisition to enhance the spectra sensitivity. ^{29}Si MAS NMR spectra were acquired at 79.46 MHz with $\pi/2$ pulse width of 4.6 μs and a recycle delay of 200 s. The $\pi/2$ pulse lengths for ^1H and ^7Li were typically 4 and 6 μs, respectively. Typically, a repetition time of 5 s was used in all the NMR experiments. The ^{29}Si, ^{13}C and ^1H chemical shifts were externally referenced to tetramethylsilane (TMS) at 0.0 ppm. ^7Li chemical shifts were referenced to solid LiCl.

Alternating current impedance measurements of the samples were performed using a CH Instrument Model 604A Electrochemical Analyzer (CH Instruments, Inc., USA) under an oscillation potential of 10 mV from 100 kHz to 10 Hz. All the thin hybrid electrolyte films were sandwiched by two polished stainless steel blocking electrodes for conductivity tests. The presenting ionic conductivity values (σ) are obtained from the relationship, $\sigma = t/(R_bA)$, where R_b is the bulk electrolyte resistance, t is the thickness, and A is the area of the sample.

3. Results and discussion

In this study, a series of the crosslinked organic–inorganic hybrid electrolytes were prepared on the basis of poly(ethylene glycol) diglycidyl ether (PEGDE) blended with 3-glycidoxypropyltrimethoxysilane (GPTMS) in the presence of lithium perchlorate ($LiClO_4$) acting as ionic source and oxirane ring-opening catalyst. It is noted that when surrounded by PEG chain or polarizable ether oxygen, the lithium ion of the more dissociable perchlorate salt closely resembles the alkali-metal ion complexed with crown ether, which is known to be an effective catalyst for anionic polymerization [21,22]. In the present curing system, this pseudo crown ether lithium ion complex seems to play a role of initiating the ring-opening reaction of the epoxide group through attacking the carbon–oxygen bond of the oxirane ring, causing the formation of an alkoxide ion. Thus, the initiated epoxide homopolymerization proceeds, resulting in oligo- or poly(ethylene oxide) derivatives [23]. Further, the methoxysilane groups ($\equiv$Si–OCH_3) on GPTMS can be hydrolyzed into silanol groups ($\equiv$Si–OH) by the moisture in air in the presence of tin-catalyst and subsequently can undergo self-condensation reactions to produce siloxane bonds ($\equiv$Si–O–Si$\equiv$) [24,25]. Epoxide cross-linking and inorganic polymerization are therefore concomitant processes, and consequently organic polymer chains are covalently linked to inorganic domain. The schematic structure of hybrid networks is shown in Scheme 1. The apparent mechanical property of the obtained hybrid material strongly depends upon the weight ratio of PEGDE/GPTMS used and the amounts of lithium salt added. Brittle hybrids are obtained for the existence of smaller amounts of PEGDE in the material matrix, whereas very soft gummy resins are obtained for higher amounts of PEGDE. The resulted hybrid electrolytes with the weight ratio of PEGDE/GPTMS to be 2.0 are observed to be transparent and elastic over the investigated amounts of $LiClO_4$.

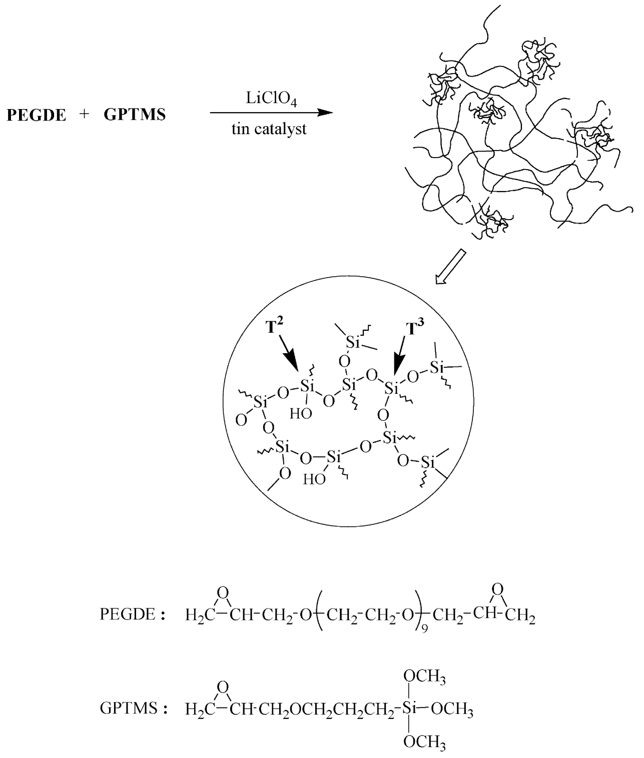

Scheme 1. Schematic structure of the organic–inorganic hybrids doped with $LiClO_4$, PEGDE-GPTMS-$LiClO_4$.

3.1. FT-IR studies

Infrared spectroscopy is a convenient method to have an insight into the development of an organic–inorganic network, and also can be employed to further elucidate the complex interplay between ionic transport process and interionic interactions. Fig. 1 shows the FT-IR spectra of PEGDE-GPTMS-$LiClO_4$ complexes with various $LiClO_4$ concentrations ranged from 0.1 to 5 mmol $LiClO_4$/g PEGDE. It is clearly shown that the characteristic absorption bands for the –OH and –C–O–C– stretching vibrations at 3700–3150 (Fig. 1(a)) and 1200–1050 cm^{-1} (Fig. 1(b)), respectively. The absorption band at $\sim 1034\ cm^{-1}$ is the asymmetric stretching of Si–O–Si, and that at 960–950 cm^{-1} is the band of Si–OH. A broad band at $\sim 880\ cm^{-1}$ is also observed, which is the characteristic of the metal-oxygen breathing motion, and evidences for the formation of PEO salt and crown ether complexes [26,27]. The bands located between 810 and 790 cm^{-1} are attributed to the vibrations of the silica

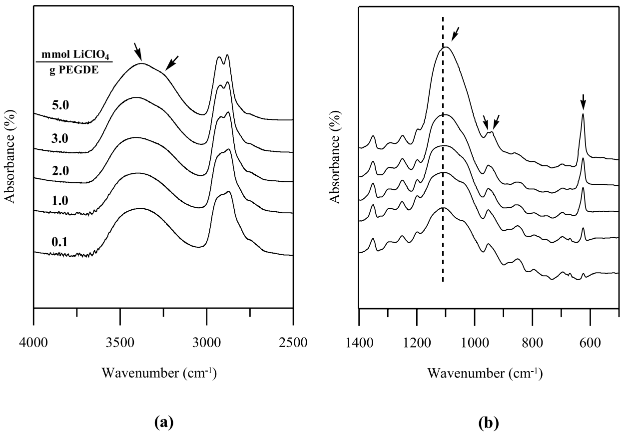

(a) (b)

Fig. 1. FT-IR spectra recorded of PEGDE-GPTMS doped with various $LiClO_4$ concentrations in the frequency range from (a) 4000 to 2500 cm^{-1}, and (b) 1400 to 500 cm^{-1}.

network [28]. The band at $\sim 625\ \mathrm{cm}^{-1}$ is assigned to the vibration modes of $\mathrm{ClO_4^-}$ ion [29]. As evidenced in Fig. 1, it is obvious that when the concentration of $\mathrm{LiClO_4}$ salt increases in the hybrid complexes, the frequencies and intensities of the stronger bands change significantly, indicating that the introduction of salt into the polymer network can change the intermolecular interactions. For the salt concentration of 5.0 mmol $\mathrm{LiClO_4}$/g PEGDE (Fig. 1(b)), a sharp band at $\sim 942\ \mathrm{cm}^{-1}$ due to the symmetric $\mathrm{ClO_4^-}$ stretching vibration for solvent-separated ion pairs $[\mathrm{Li(PEG)}_n\mathrm{ClO_4^-}]_8$ [30,31] is obviously observed.

Fig. 1(a) shows the –OH stretching region of the FT-IR spectra of the organic–inorganic hybrid networks with different amounts of $\mathrm{LiClO_4}$ salt. A slightly progressive shift in the maximum of hydroxyl stretching band to lower wavenumber with increasing $\mathrm{LiClO_4}$ concentration is observed. In addition, a further hydroxyl stretching vibration is detected around $3250\ \mathrm{cm}^{-1}$ for each polymer complex, which can be ascribed to the –OH stretching vibration of the hydroxyls hydrogen-bonded to perchlorate ions ($\mathrm{ClO_4^-}$) [32]. Changes in FT-IR can be ascribed to the interactions between hydroxy groups and ions. Since an ion-dipole interaction is stronger than a dipole–dipole interaction, a negative shift in the wavenumber takes place.

Two FT-IR regions of C–O–C symmetric and asymmetric stretching vibrations observed at $\sim 1100\ \mathrm{cm}^{-1}$, and ν_4 ($\mathrm{ClO_4^-}$) envelope ones occurring at $\sim 625\ \mathrm{cm}^{-1}$ are of particular interest in our studies. Changes in the intensity, shape, and position of the C–O–C stretching mode are associated with the polyether-$\mathrm{LiClO_4}$ interactions, whereas ν_4 ($\mathrm{ClO_4^-}$) stretch is associated with ion–ion interactions in these electrolytes. In Fig. 1(b), the slightly decrease in the position of the C–O–C stretch maximum and the broadening of this band are observed with an increase in the salt concentration, confirming the interactions between polyether and salt. The downshift of the maximum of the C–O–C mode is due to the formation of transient cross-links which weaken the C–O polyether bonds. To study the ion–ion interactions, the spectral features of ν_4 ($\mathrm{ClO_4^-}$) mode appearing at $\sim 625\ \mathrm{cm}^{-1}$ were fitted with a Gaussian–Lorentzian function using Grams 386 deconvolution software (Galatic). The enlarged ν_4 ($\mathrm{ClO_4^-}$) envelope can be separated into two contributions with the maximum at ~ 624 and $\sim 633\ \mathrm{cm}^{-1}$, as shown in Fig. 2(a). The band centered at $\sim 624\ \mathrm{cm}^{-1}$ has been assigned to the 'free' $\mathrm{ClO_4^-}$ anion vibrations and the band centered at $\sim 633\ \mathrm{cm}^{-1}$ to the vibration of $\mathrm{Li^+ClO_4^-}$ contact-ion pairs [33].

As seen in Fig. 2(a), only single well-fitted mode with a maximum at $\sim 624\ \mathrm{cm}^{-1}$ exists at the salt concentration of 0.1 mmol $\mathrm{LiClO_4}$/g PEGDE, indicating the majority of the $\mathrm{ClO_4^-}$ exists as spectroscopically 'free' species; meanwhile, the opposite $\mathrm{Li^+}$ cations accept the electrons from ether oxygens of hybrid network in an 'acceptor–donor' configuration. (See ^{7}Li MAS NMR). Fig. 2(b) shows the fraction of 'free' anions as a function of salt concentration for the PEGDE-GPTMS-$\mathrm{LiClO_4}$ electrolytes, in which the fraction is calculated as the ratio of the area under the $\sim 624\ \mathrm{cm}^{-1}$ mode to the total area under the ν_4 ($\mathrm{ClO_4^-}$) envelope. As evidenced in Fig. 2(b), the fraction of 'free' anions decreases with increasing salt concentration and levels off at the salt concentration of 2.0–3.0 mmol $\mathrm{LiClO_4}$/g PEGDE, then slightly increases for higher salt concentrations. Upon addition of salt, more and more free ions become bound with the opposite ions to form contact ions, and hence the content of the free ions decreases. In the concentrated salt concentrations, the redissociation of 'free' ions might be occurred due to an increase in the system permittivity or dipole–dipole interactions, as previously suggested by several authors [34].

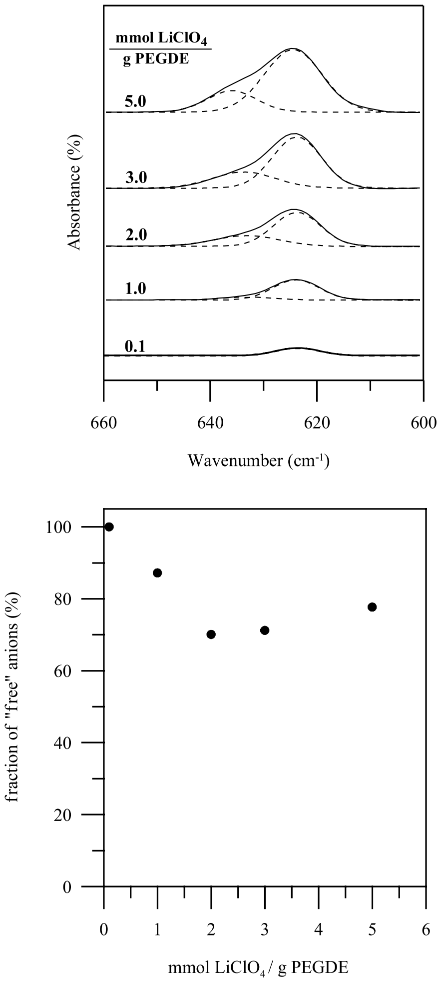

Fig. 2. (a) Deconvoluted spectra of the ν_4 ($\mathrm{ClO_4^-}$) FT-IR region for PEGDE-GPTMS doped with various $\mathrm{LiClO_4}$ concentrations; (b) fraction of spectroscopically 'free' anions as a function of salt concentration for PEGDE-GPTMS-$\mathrm{LiClO_4}$.

3.2. DSC and TGA studies

DSC was utilized to examine the effect of $\mathrm{LiClO_4}$ on the morphologically based thermal transitions of the polyether-siloxane hybrid electrolytes. Fig. 3 displays the DSC thermograms for PEGDE-GPTMS-$\mathrm{LiClO_4}$ electrolytes

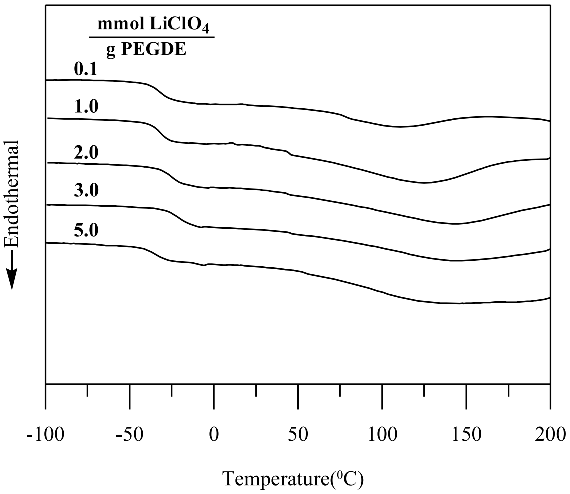

Fig. 3. DSC curves for PEGDE-GPTMS-$LiClO_4$ complexes with various $LiClO_4$ concentrations (mmol $LiClO_4$/g PEGDE).

with various salt concentrations at the weight ratio of PEGDE/GPTMS = 2.0. The results of thermal measurements are summarized in Table 1. As seen in Fig. 3, no first-order transitions corresponding to the melting of the crystalline PEG phase at ~70 °C is observed indicating that no existence of crystalline PEO phase in these composite electrolytes. These DSC traces also demonstrate the presence of two second-order transitions for all the samples. These two transitions could be associated with the biphasic character of the polyether chains inside the hybrid networks [35]. The polymer far away from silica networks behaves as unrestricted polyether chains, possessing glass transition temperature (T_{g1}) in the negative temperature region where changing with the amounts of salt added. On the contrary, the polymer near the silica nodes is more rigid due to physical interaction or covalent bond with silica, showing transition at around 50 °C, T_{g2}.

As seen in Table 1, the T_{g1} increases as the salt is added and reaches a maximum for 3.0 mmol $LiClO_4$/g PEGDE. This is due to the formation of transient cross-links between the lithium cation and the polyether segment. However, the T_{g1} decreases at the salt concentration of 5.0 mmol $LiClO_4$/g PEGDE. Table 1 also lists the value of glass transition zone of $T_{g1}(\Delta T_{g1})$ varied with the $LiClO_4$ uptake. This value reaches a minimum at salt concentration of 1.0 mmol $LiClO_4$/g PEGDE and thereafter shows a increasing trend. The glass transition zone is defined as the difference between the onset and endset temperatures of thermal transition process and reflects the number of relaxation processes associated with the transition. Complexed polyether units may be located randomly along the polyether segments. The mutual influences on the behaviors of the free and complexed polyether units probably undergo relaxation processes with different relaxation times, resulting in the broadening of the glass transition. At a relatively high $LiClO_4$ concentration, almost all polyether units are complexed with $LiClO_4$, and thus the distribution of the relaxation times becomes narrow again. In the concentrated salt concentration, the strong ion–ion interactions must exist. Consequently, the less mobile ion pairs and clusters are predicted to form. Such ion cluster transient cross-linkers probably not only interrupt the interaction between lithium cation and ether oxygen but also increase the distance between the polymer chains, leading to the so-called plasticizing effect [36]. Hence, these effects can be used to explain why a decrease in T_{g1} is observed at the salt concentration of 5.0 mmol $LiClO_4$/g PEGDE, and the ΔT_{g1} increases at higher salt concentrations. As the salt concentration increases, moreover, the endothermic feature develops with a maximum in the range of 110–150 °C. This endothermic peak is ascribed to the melting temperature of the crystalline PEG-$LiClO_4$ complex phase (T_{mc}). Besides, as evidenced in Fig. 3 and Table 1, the portion of PEG-$LiClO_4$ complex phase and the corresponding T_{mc} increase with further addition of salt.

TGA is used to measure the thermal stability of hybrid electrolytes. Fig. 4 shows the weight loss behaviors of the PEGDE-GPTMS-$LiClO_4$ electrolytes investigated by TGA scanning from 100 to 800 °C under nitrogen. As can be seen in Fig. 4, the hybrid electrolyte with the lowest salt concentration (0.1 mmol $LiClO_4$/g PEGDE) decomposes in a single step and the temperature of initial 10% weight loss ($T_d^{0.1}$) occurs at around 340 °C. With further addition of salt, the creation of a second stage reflects the salt/polymer complex degradation, and their further degradation rate of weight loss tends to increase remarkably with increasing $LiClO_4$ salt concentration. This behavior may be explained by the weakness of C–O bond, caused by the decreased electronic density due to the O–Li^+ interaction. Alternatively,

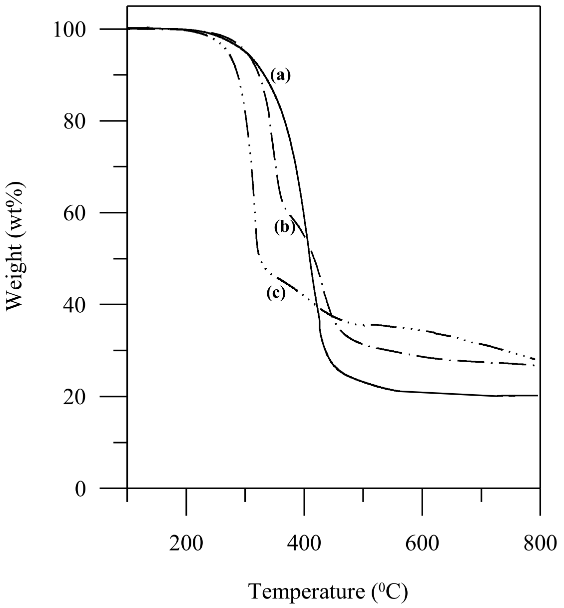

Fig. 4. TGA thermograms for PEGDE-GPTMS-$LiClO_4$ complexes with various $LiClO_4$ concentrations under nitrogen atmosphere: (a) 0.1, (b) 1.0, and (c) 3.0 mmol $LiClO_4$/g PEGDE.

perchlorate oxidation of polyether phase can cause this thermal event starting from ~500 °C.

3.3. ^{29}Si MAS NMR

Solid-state ^{29}Si MAS NMR spectroscopy was used to characterize the silicon condensation and to indicate the silica network architecture inside these materials. It is well established [37] that the hydrolytic condensation of monosubstituted silanes can result in numerous products, generally referred to as silsesquioxanes, of which the molecular structures are altered with the substituent groups and the reaction conditions employed. Fig. 5 shows the ^{29}Si MAS NMR spectra of the PEGDE-GPTMS hybrids doped with various amounts of $LiClO_4$. As seen in this figure, only two major peaks at around −67 and −58 ppm are observed. The positions of these signals are agreement with those of siloxane fragments in T^3 ($RSi^*(OSi)_3$) and T^2 ($RSi^*(OSi)_2$-OH) arrangements, respectively (where R is the organic motif). Furthermore, these spectra do not show any evidence of peaks associated to T^0 species, namely uncondensed materials trapped in this hybrid network. Fig. 5 also shows that the intensity of the T^3 resonance is much higher than that of T^2, providing a predominating content of the three-dimensional silsesquioxane network on the inorganic side, and the formation of silica nodes which act as cross-linking units of the polymeric PEO network. In addition, the added amount of $LiClO_4$ has somewhat influenced on the hydrolysis-condensation process of the alkoxysilane on GPTMS, particularly for the salt concentration of 5.0 mmol $LiClO_4$/g PEGDE.

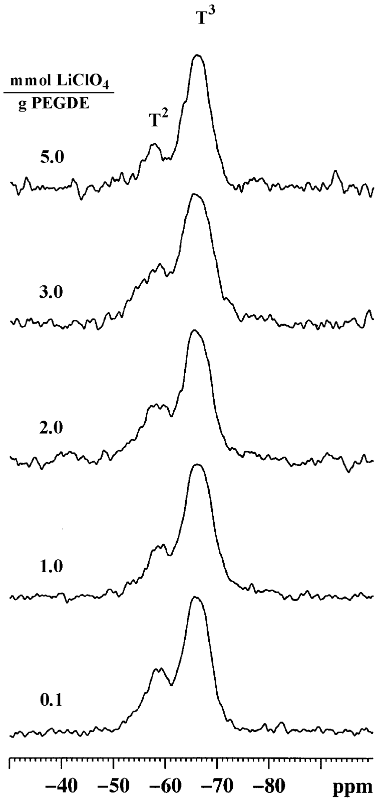

Fig. 5. ^{29}Si MAS NMR spectra of PEGDE-GPTMS-$LiClO_4$ complexes doped with various $LiClO_4$ concentrations.

The condensation degree (cd) of alkoxysilane (percentage of siloxane bonds formed) can be calculated according to the general equation $cd = 0.66[0.5(T^1 \text{ area}) + 1.0(T^2 \times \text{area}) + 1.5(T^3 \text{ area})]$, and the obtained results are summarized in Table 2. As seen in Fig. 5, a signal broadening can be observed with increasing salt concentration up to 3.0 mmol $LiClO_4$/g PEGDE. This broadening is due to the packing of these units in different environments and is related to a structural restricted mobility. As seen in Table 2, notably, the highest cd of alkoxysilane is observed at the highest salt concentration (5.0 mmol $LiClO_4$/g PEGDE). This observation is connected to the higher mobility of the matrix due to the plasticizing effect at this salt concentration, which is needed for a high degree of condensation.

3.4. ^{1}H MAS NMR

Solid-state ^{1}H spectra usually result in broad unresolved peaks under MAS with moderate spinning speed, however, mainly containing information about molecular dynamics. The ^{1}H MAS NMR spectra of PEGDE-GPTMS hybrids, acquired at room temperature, doped with various amounts of $LiClO_4$ are presented in Fig. 6. As evidenced in this figure, two peaks corresponding to the methylene protons adjacent to ether oxygens are observed at approximately 3.7 and 4.3 ppm, respectively. Upon addition of $LiClO_4$ up to 3.0 mmol $LiClO_4$/g PEGDE, a line broadening and an increase in the relative intensity of the left-shoulder peak are observed. This might be resulted from the complexation of Li cations with the ether oxygens in the polymer chains, which largely reduces the mobility of the polymer chain. However, the reduced peak linewidth and the relative intensity of the left-shoulder are clearly observed at the highest amounts of lithium salt, and could be ascribed to the plasticizing effect, as above explained.

3.5. ^{13}C CP/MAS NMR

^{13}C CP/MAS NMR spectra were carried out at different $LiClO_4$ concentrations in order to analyze the effect of the

Table 2
The deconvolution results for ^{29}Si MAS NMR

mmol $LiClO_4$/g PEGDE	Percentage (%)		cd[a]
	T^2	T^3	
0.1	39.0	61.0	86.1
1.0	27.9	72.1	89.8
2.0	37.8	62.2	86.5
3.0	36.1	63.9	87.1
5.0	24.3	75.7	91.0

[a] cd: condensation degree of alkoxysilane.

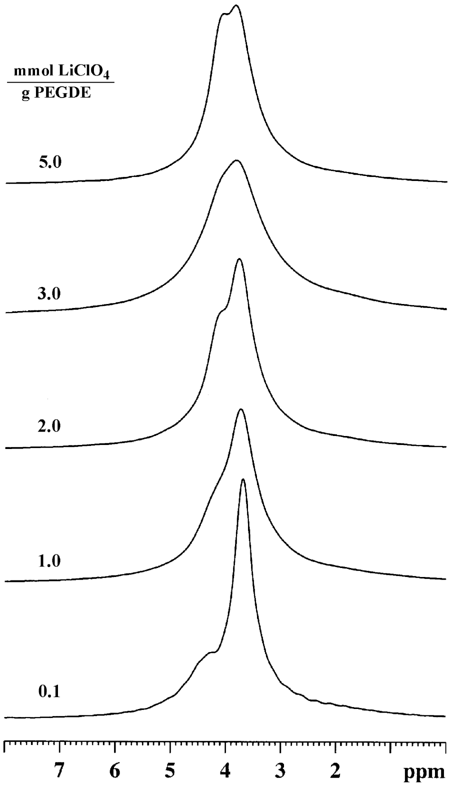

Fig. 6. ^{1}H MAS NMR spectra of PEGDE-GPTMS-LiClO$_4$ complexes doped with various salt concentrations.

amount of lithium salt on the structure of composite hybrids and to study the chemical process involved Fig. 7 shows the ^{13}C CP/MAS NMR spectra of the PEGDE-GPTMS hybrids doped with various amounts of LiClO$_4$. For the sample doped with the salt concentration of 0.1 mmol LiClO$_4$/g PEGDE, one weak peak at 44 ppm for the carbon atom of oxirane ring is still observed, indicating the incompleteness of the ring opening. Two peaks at 10 and 24 ppm are assigned to the methylene carbons in α and β position to the silicon atom, respectively. The peak at ca. 70 ppm is due to those methylene carbons adjacent to ether oxygen. Upon addition of salt except the salt concentration of 5.0 mmol LiClO$_4$/g PEGDE, the peak corresponding to the epoxide ring disappears, associated with the ring opening of epoxide catalyzed by LiClO$_4$. Beside, the line broadening and the displacement to lower ppm values are observed with the peak of methylene carbons adjacent to ether oxygen (see inset for comparison). These behaviors are due to the interactions between Li$^+$ cations and the ether oxygens in the hybrids. For the more concentrated lithium salt environment (5.0 mmol LiClO$_4$/g PEGDE), the line narrowing and the unobvious upfield chemical shift for the peak at ca.70 ppm as well as the peak for oxirane ring at 44 ppm are observed. This is suggested that the existence of plasticizing effect leads to the higher mobility of the matrix and an insufficient amount of dissociated LiClO$_4$ to ensure the completion of epoxide ring opening. Another, the peaks at 64 and 59 ppm due to the formation of diol function and methyl ether terminal group, respectively [38], are not obviously seen in these spectra, suggesting that these reactions are the minor ones for the interionic complex formation.

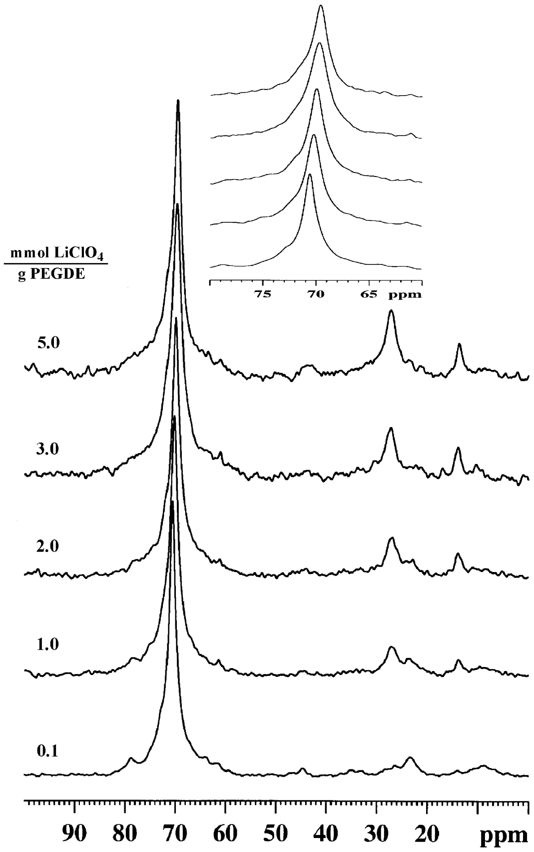

Fig. 7. ^{13}C CP/MAS spectra of PEGDE-GPTMS-LiClO$_4$ complexes doped with various salt concentrations. The ether carbon region is enlarged as shown in the inset.

3.6. ^{7}Li MAS NMR

To gather information regarding the Li cationic environment, high-resolution ^{7}Li MAS techniques with high-power proton decoupling were employed [39]. It is well known that the lineshape and width of solid-state NMR spectra are strong temperature-dependent due to the motion-dependent anisotropic nuclear spin interactions. As raising the temperature, the molecular motion is accelerated and the anisotropy is averaged, then the motional narrowing in the lineshape will occur. In order to have an insight into the immediate environments of Li$^+$ ions, therefore, the proton-decoupled ^{7}Li MAS NMR spectra of PEGDE-GPTMS-LiClO$_4$ complexes as a function of salt concentration, recorded at −60 °C lower than their T_{g1}, are displayed in Fig. 8, together with the decomposed spectra by the least-squares fit between the experimental and the calculated spectra to reveal the composition of individual lithium species. As evidenced in this figure, only one resonance centered at −0.91 ppm (site I) is observed in the case of

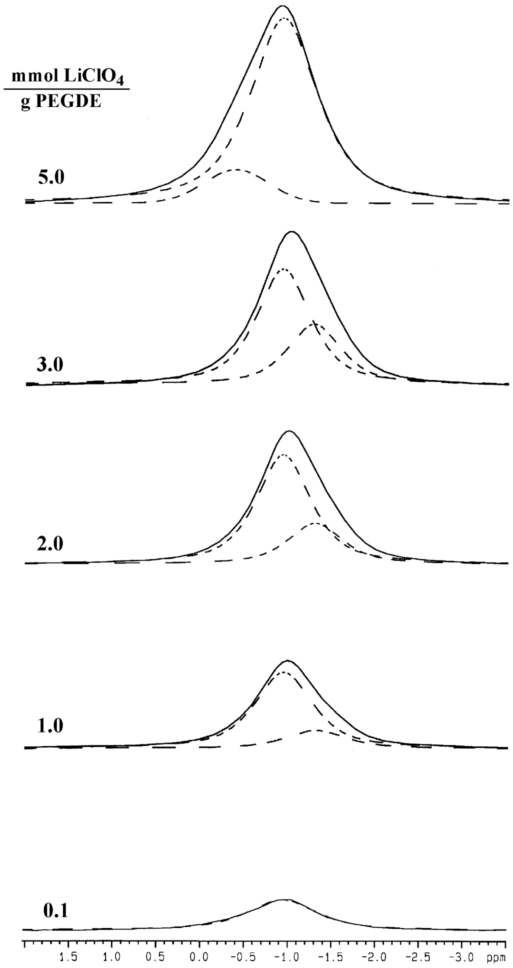

Fig. 8. ^{7}Li proton-decoupled MAS NMR spectra of PEGDE-GPTMS-$LiClO_4$ complexes doped with various salt concentrations at −60 °C at a spinning speed of 3 kHz, along with the deconvolution (dashed lines).

0.1 mmol $LiClO_4$/g PEGDE. With increasing $LiClO_4$ concentration up to 3.0 mmol $LiClO_4$/g PEGDE, the lineshapes are asymmetric, and a shoulder (site II) lying at ca. −1.30 ppm becomes visible and shows a concentration-dependence of its intensity. This indicates that at least two major lithium conformations are directly visible, although they are only partially resolved, i.e. at least two distinct lithium species with different local environments existing in the hybrid complexes. Furthermore, the low dielectric constant environment of polymer electrolytes presumably is conducive to the formation of ion pairs even higher order ionic aggregates [40], and the un-dissociated $LiClO_4$ salt shows a broad lithium resonance at ca. −2.4 ppm under the same experimental conditions. Thus it is rational to conclude that site I is assigned to the Li^+ cations coordinated with ether oxygens in polyether chains, while site II is associated with the ion pairs or aggregates. In the ultraconcentrated medium (5.0 mmol $LiClO_4$/g PEGDE), on the other hand, these two sites are not resolved, and only a broad resonance is observed. In the meantime, a new peak (site III) located at −0.38 ppm is observed. Such a downfield peak may include a range of anion–cation-polyether coordination possibilities with different modes for different combination of anions and/or ether oxygens, and could be assigned to the solvent-separated lithium species of higher order ion aggregates. This is supported by the earlier analysis of FT-IR results and the argument for the plasticizing effect when the salt concentration reaches the 5.0 mmol $LiClO_4$/g PEGDE.

3.7. Ionic conductivity

Fig. 9 shows the temperature dependence of ionic conductivity (σ) of the PEGDE-GPTMS hybrids doped with various $LiClO_4$ concentrations. As seen in this figure, it is evident that variation of conductivity with temperatures follows the VTF-like relationship [41], which is indicative of ionic conductivity being coupled to polymer segmental motion. The effect of salt concentration on ionic conductivity can be illustrated by examining isothermal plots as shown in Fig. 10. As the $LiClO_4$ concentration increases, the changes in free volume, electrostatic interactions, and hydrogen bonding significantly affect conductivity. From the conductivity data (Figs. 9 and 10), it is clear that these ion transport behaviors cannot be explained by only the effect of the ionic mobility or of the number of carrier ions but are affected by the combination of these two effects.

As shown in Fig. 10, at lower temperatures (<55 °C), a maximum conductivity is observed at 2.0 mmol $LiClO_4$/g PEGDE in the salt concentrations ranging from 0.1 to 5.0 mmol $LiClO_4$/g PEGDE. This suggests that the effects of increasing charge carrier density are overcome by the accompanying decrease in segmental mobility and the

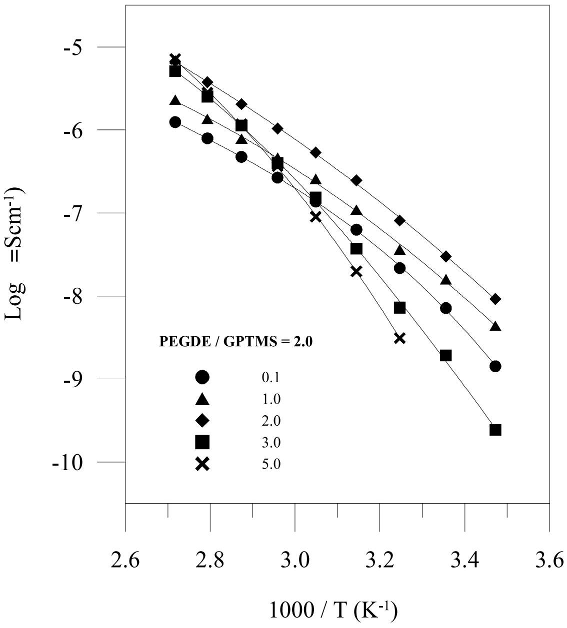

Fig. 9. Temperature dependence of ionic conductivity of PEGDE-GPTMS-$LiClO_4$ complexes doped with different amounts of $LiClO_4$.

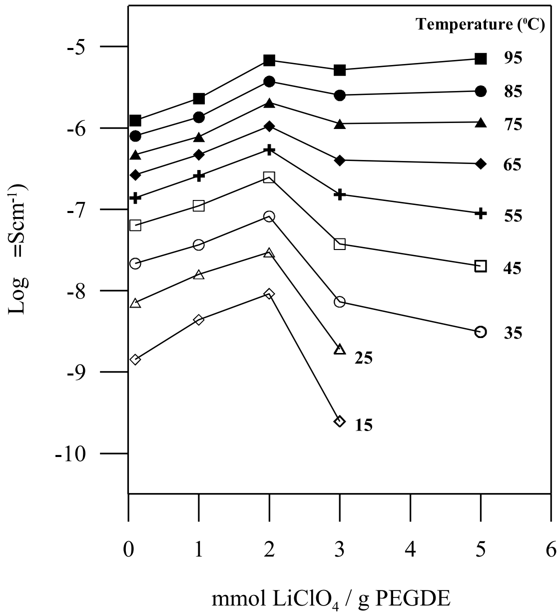

Fig. 10. Salt concentration dependence of ionic conductivity under various temperatures from 15 to 95 °C.

increase in ionic association. The decrease in segmental mobility arising from transition cross-linking and the increase of ionic association leading to the formation of ion pairs or aggregates are verified by the earlier FT-IR, DSC and ^{7}Li NMR studies. At lower salt concentration level (below 2.0 mmol $LiClO_4$/g PEGDE), the extent of contact ion pairs is low, and consequently the conductivity is dominated by the number of charge carriers. At a relatively high $LiClO_4$ concentration, the formation of ion pairs or aggregates decreases the number density of charge carriers present, and also limit the mobility of the charge carriers throughout the polymer matrix; both effects result in a reduction in bulk ionic conductivity.

Furthermore, at higher temperatures, the trend of ionic conductivity data passed through a maximum is different from that at lower temperatures. Watanabe et al. [42] reported the equations to quantitatively express the temperature dependence of the ionic conductivity for the polymer complexes formed by PPO-urethane networks and $LiClO_4$, where the conductivity was correlated with the ionic mobility and carrier ions. The main contributing term to the difference in the conductivity at lower temperatures in Fig. 10 can also be deduced to the ionic mobility. Since $(T - T_{g1})$ for each sample is different changing with the $LiClO_4$ concentration. At higher temperatures, the term $(T - T_{g1})$ for the complexes with different $LiClO_4$ concentration does not change with the concentration as greatly as it does at lower temperatures, and result in similar ionic mobility. Thus, the conductivity is mainly influenced by the difference of the concentration of carrier ions, in agreement with the interpretation based on the above-mentioned results.

4. Conclusions

A chemical-covalently polyether-siloxane hybrid electrolyte based on epoxide network formed by curing PEDGE and GPTMS in the presence of $LiClO_4$ has been prepared. Specific interactions among ions and polymer host have been examined via the application of FT-IR, DSC and ^{7}Li MAS NMR and are detected due to the presence of the interaction of hydrogen-bonded clusters around ClO_4^- ions, Li^+ cations coordinated with oxygen ligands of the polyether chains and ionic association. Furthermore, solid-state ^{13}C NMR spectra demonstrate that an appropriate amount of dissociated $LiClO_4$ is necessary to ensure the completion of epoxide ring opening. The ion conduction follows VTF-like temperature dependence. These combined experiments show that a strong correlation between the behaviors of the composite polymer electrolytes and the ionic species.

Acknowledgements

The authors would like to thank the National Science Council, Taipei, ROC. for their generous financial support of this research. The authors highly appreciated Ms. Ru-Rong Wu for her profound contribution in NMR experiments.

References

[1] MacCallum JR, Vincent CA, editors. Polymer electrolyte reviews, vols. 1 and 2. London: Elsevier; 1987/1989.
[2] Gray FM. Solid polymer electrolytes-functional and technological applications. Weinheim, Germany: VCH; 1991.
[3] Scrosati B. Application of electroactive polymers. London: Chapman and Hall; 1993.
[4] Scrosati B. Mater Sci Engng 1992;B12:369.
[5] Berthier C, Gorecki W, Minier M, Armand MB, Chabagno JM, Rigaud P. Solid State Ionics 1983;11:91.
[6] Boden N, Leng SA, Ward IM. Solid State Ionics 1991;45:261.
[7] Lightfoot P, Mehta A, Bruce PG. J Mater Chem 1992;2:379.
[8] Sun HY, Sohn HJ, Yamamoto O, Takeda Y, Imanishi N. J Electrochem Soc 1999;146:1672.
[9] Croce F, Appetecchi GB, Persi L, Scrosati B. Nature 1998;394:456.
[10] MacFarlan DR, Newman PJ, Nairn KM, Forsyth M. Electrochim Acta 1998;43:1333.
[11] Ravaine D, Seminel A, Charbouillot Y, Vincens M. J Non-Cryst Solids 1986;82:210.
[12] Judeinstein P, Livage J, Zarudianski A, Rose R. Solid State Ionics 1988;28–30:1722.
[13] Popall M, Durand H. Electrochim Acta 1992;37:1593.
[14] de Zea Bermudez V, Alcacer L, Acosta JL, Morales E. Solid State Ionics 1999;116:197.
[15] de Souza PH, Bianchi RF, Dahmouche K, Judeinstein P, Faria RM, Bonagamba TJ. Chem Mater 2001;13:3685.
[16] Dahmouche K, Atik M, Mello NC, Bonagamba JT, Panepucci H, Aegerter M, Judeinstein P. Mater Res Symp Proc 1996;435:363.
[17] Dahmouche K, de Souza PH, Bonagamba JT, Panepucci H,

Judeinstein P, Pulcinelli SH, Santilli CV. J Sol–Gel Sci Technol 1998;13:909.

[18] Fujinami T, Mehta A, Sugie K, Mori K. Electrochim Acta 2000;45: 1181.

[19] Nishio K, Okubo K, Watanabe Y, Tsuchiya T. J Sol–Gel Sci Technol 2000;19:187.

[20] Dahmouche K, Santilli CV, Silva MD, Ribeiro A, Pulcinelli SH, Craievich AF. J Non-Cryst Solids 1999;247:108.

[21] Stolarzewicz A, Grobelny Z. Makromol Chem 1992;193:531.

[22] Wu S, Peng X, Song Y, Zhou Z, Lin Y, Chen D, Wang F. Solid State Ionics 1995;76:163.

[23] Dusek K, Epoxy resins and composites I, New York: Springer-Verlag; 1985.

[24] Hou SS, Kuo PL. Polymer 2001;42:9505.

[25] Liang WJ, Kuo PL. J Polym Sci, Polym Chem Ed 2004; in press.

[26] Papke BL, Ratner MA, Shriver DF. J Phys Chem Solids 1981;42:493.

[27] Eschmann J, Strasser J, Xu M, Okamoto Y, Eyring E, Petrucci S. J Phys Chem 1990;94:3908.

[28] Kioul A, Mascia L. J Non-Cryst Solids 1994;175:169.

[29] Cohen H. J Chem Soc 1952;4282.

[30] Yamanaka S, Sarubo M, Tadanobu K, Hattori M. Solid State Ionics 1992;57:271.

[31] James DW, Mayes RE. Aust J Chem 1982;35:1775.

[32] Symons MCR, Kevan L, Webster BC, editors. Electron-solvent and ion-solvent interactions. New York: Elsevier; 1976. p. 311–41.

[33] Salomon M, Xu M, Eyring EM, Petrucci S. J Phys Chem 1994;98: 8234.

[34] Petrucci S, Eyring EM. J Phys Chem 1991;95:1731. and the references therein.

[35] Mello NC, Bonagamba TJ, Panepucci H, Dahmouche K, Judeinstein P, Aegerter MA. Macromolecules 2000;33:1280.

[36] van Heumen JD, Stevens JR. Macromolecules 1995;28:4268.

[37] Baney RH, Itoh M, Sakakibara A, Suzuki T. Chem Rev 1995;95:1409.

[38] Templin M, Wiesner U, Spiess HW. Adv Mater 1997;9:814.

[39] Lin CL, Kuo PL, Wu RR, Kao HM. Macromolecules 2002;35:3083.

[40] (a) Marcus Y. Ion solvation. New York: Wiley; 1985. p 180–184. (b) Davies CW. Ion association. Washington: Butterworths; 1962. p 150–161.

[41] (a) Gray FM. Polymer electrolytes. UK: The Royal Society of Chemistry; 1997. Chapter 2. (b) Vogel H. Phys Z 1921;22:645. (c) Tamman G, Hesse W. Z Anorg Allg Chem 1926;156:245. (d) Fulcher GS. J Am Ceram Soc 1925;8:339.

[42] Watanabe M, Sanui K, Ogata N, Kobayashi T, Ohtaki Z. J Appl Phys 1985;57:123.